

Geophysical Research Letters[®]



RESEARCH LETTER

10.1029/2023GL104159

Key Points:

- Tropical easterly wave (TEW) impact on the rainfall diurnal cycle over Costa Rica is documented in surface meteorological and sounding data
- Convectively active phases of tropical easterly waves are associated with increased hourly rainfall frequency of occurrence
- Rainfall intensity sensitivity to TEW phase is more subtle, with indications of delayed active phase peak intensity

Supporting Information:

Supporting Information may be found in the online version of this article.

Correspondence to:

B. R. Lintner,
lintner@envsci.rutgers.edu

Citation:

Wiggins, R. M., Lintner, B. R., Serra, Y. L., Durán-Quesada, A. M., Garbanzo-Salas, M., Hernández-Deckers, D., & Torri, G. (2023). Tropical easterly waves over Costa Rica and their relationship to the diurnal cycle of rainfall. *Geophysical Research Letters*, 50, e2023GL104159. <https://doi.org/10.1029/2023GL104159>

Received 21 APR 2023
Accepted 5 OCT 2023

Tropical Easterly Waves Over Costa Rica and Their Relationship to the Diurnal Cycle of Rainfall

Rani M. Wiggins¹, Benjamin R. Lintner^{1,2} , Yolande L. Serra³ , Ana María Durán-Quesada^{4,5,6} , Marcial Garbanzo-Salas⁴ , Daniel Hernández-Deckers⁷ , and Giuseppe Torri⁸ 

¹Department of Environmental Sciences, Rutgers University, The State University of New Jersey, New Brunswick, NJ, USA, ²Institute of Earth, Ocean, and Atmospheric Sciences, Rutgers University, The State University of New Jersey, New Brunswick, NJ, USA, ³Cooperative Institute for Climate, Ocean, & Ecosystem Studies, University of Washington, Seattle, WA, USA, ⁴Escuela de Física, Universidad de Costa Rica, San José, Costa Rica, ⁵Centro de Investigación en Contaminación Ambiental, Universidad de Costa Rica, San José, Costa Rica, ⁶Centro de Investigaciones Geofísicas, Universidad de Costa Rica, San José, Costa Rica, ⁷Departamento de Geociencias, Universidad Nacional de Colombia, Bogotá, Colombia, ⁸Department of Atmospheric Sciences, University of Hawai'i at Mānoa, Honolulu, HI, USA

Abstract Using an index of tropical easterly wave (TEW) activity derived from spacetime-filtered outgoing longwave radiation, we construct composites of long-term hourly surface meteorological observations and morningtime sounding data collected near San José, Costa Rica to investigate how TEWs affect the diurnal cycle of rainfall over land. Our results indicate that TEWs enhance the frequency of occurrence of rain during convectively active conditions over the course of the diurnal cycle. By contrast, rainfall conditional intensity sensitivity to TEW phase appears more nuanced, with indications that active conditions induce a slight delay in the timing of the diurnal peak intensity but a longer duration of heavier rainfall. Analysis of associated hourly surface meteorology along with sounding profiles and derived thermodynamic parameters points to both initial vertical and time-evolving surface conditions regulating diurnal behavior, such as greater instability and higher precipitable water in morningtime profiles under active phase conditions.

Plain Language Summary Over tropical land, rainfall often follows a characteristic daily (or diurnal) cycle, with a peak in the late afternoon. This study explores how tropical easterly waves, westward-propagating weather disturbances known to impact rainfall over many parts of the Tropics, affect the rainfall diurnal cycle at a long-term observation site near San José, Costa Rica. Using an index of tropical easterly wave activity, and considering the diurnal cycle in terms of rainfall occurrence frequency and intensity, the results presented here indicate generally enhanced occurrence frequency over the course of the diurnal cycle during active conditions of tropical easterly waves, while intensity shows a more nuanced behavior, with active phases showing a slight lag in peak diurnal intensity with an overall lengthening of the highest intensities. Such diurnal rainfall sensitivity to tropical easterly waves is interpreted in terms of hourly surface meteorological observations and vertical profiles from morningtime soundings.

1. Introduction

The weather over Central America, and indeed in many parts of the Tropics, is impacted by the passage of tropical easterly waves (TEWs), westward-propagating transient disturbances with spatial scales of a few thousand kilometers (e.g., Rydbeck & Maloney, 2014, 2015; Serra et al., 2008, 2010). Much of the regional interest in TEWs over the Atlantic and Eastern Pacific Ocean basins stems from their role as incipient disturbances for tropical cyclones (Hopsch et al., 2010; Thorncroft & Hodges, 2001) or as moisture sources for the North American Monsoon (Fuller & Stensrud, 2000; Higgins et al., 2004; Seastrand et al., 2015). However, it has been suggested that TEWs may be responsible for up to half of the rainfall accumulation in some regions over the tropical Americas (Dominguez et al., 2020), which in turn may significantly modulate the seasonality of rainfall over the region (Giraldo-Cardenas et al., 2022; Gomes et al., 2019; Jury, 2020). Thus, TEWs are broadly important for understanding tropical regional rainfall and its variability, including extreme rainfall events. Operationally, the Instituto Meteorológico Nacional (IMN) de Costa Rica frequently issues forecast advisories for extreme rainfall with the passage of TEWs over Central America, with upwards of 40–50 advisories per year not uncommon (IMN, 2023). Of course, more process-based knowledge of the linkage between TEWs and heavy rainfall is needed, particularly with respect to associations with hazards such as flooding and landslides.

© 2023 The Authors.

This is an open access article under the terms of the [Creative Commons Attribution-NonCommercial License](https://creativecommons.org/licenses/by-nc/4.0/), which permits use, distribution and reproduction in any medium, provided the original work is properly cited and is not used for commercial purposes.

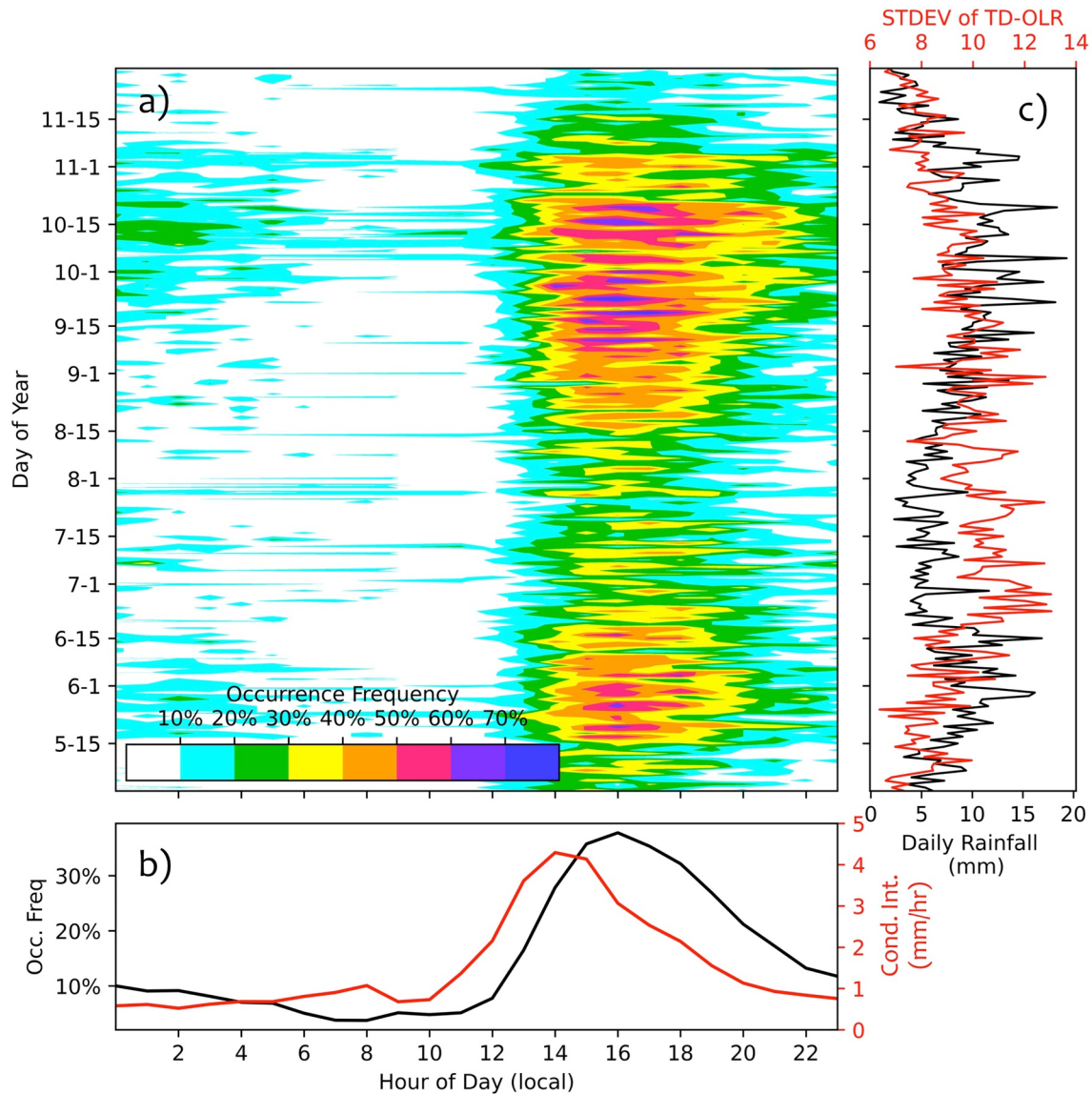


Figure 1. Climatological diurnal and seasonal rainfall characteristics at San José, Costa Rica (1995–2019). (a) Occurrence frequency of hourly rainfall by local time of day (x -axis, midnight at 0) and calendar day of year (y -axis, starting from 1 May at the bottom). (b) May–November-mean hourly occurrence frequency (black; in percent) and conditional intensity (red; in mm/hr). (c) Daily rainfall accumulation (black; in mm) along with the interannual standard deviation of the daily TD-filtered outgoing longwave radiation index (red; in $W m^{-2}$).

Many of the previous efforts to diagnose the behavior and characteristics of TEWs have focused on oceanic regions, with comparatively little attention to TEWs over land, at least outside of Africa, which is an important source region for such waves (e.g., Mekonnen et al., 2006). Coupling with the diurnal cycle is a potentially significant consideration for evaluating and interpreting the TEW-precipitation relationship over land. Indeed, as with many land regions in the Tropics (Liu & Zipser, 2008; Rapp et al., 2014; Yang & Slingo, 2001), rainfall over Costa Rica exhibits a pronounced late afternoon peak (Mora et al., 2020; see also Figure 1 below). To leading order, such diurnal phasing over land arises from interaction with the surface, as solar heating over course of the day grows and destabilizes the atmospheric boundary layer. Of course, factors such as land-ocean contrast, interactions with topography, or propagating mesoscale convective systems (MCSs) are known to modify or may even dominate local diurnal phasing (Mapes, Warner, & Xu, 2003; Mapes, Warner, Xu, & Negri, 2003; Nesbitt & Zipser, 2003; Warner et al., 2003).

In summer 2019, coordinated land-based observations, including surface meteorology, Global Navigation Satellite System precipitable water retrievals, radiosonde launches, and water isotopes in rainfall, were undertaken as

part of the Organization of Tropical East Pacific Convection (OTREC) field campaign (Fuchs-Stone et al., 2020; Huaman et al., 2022). A key objective of OTREC was to advance process understanding of the evolution of TEWs transiting Central America from the Caribbean to the Eastern Pacific, including how the potential coupling of TEWs to the diurnal cycle over land may affect the rainfall triggered by TEW passage. The present study aims to establish the climatological relationship between TEWs and the diurnal cycle of rainfall over Costa Rica to provide context for the OTREC field campaign observations.

To assess the long-term TEW-rainfall diurnal cycle relationship over Costa Rica, we use a suite of multidecadal radiosonde profiles from the World Meteorological Organization (WMO) sounding site outside San José (Alajuela), Costa Rica (WMO 78762, airport code SJO, 84.21°W, 10.00°N, 921 m.a.s.l.; see Figure S1 in Supporting Information S1) and hourly surface meteorological from IMN's Estación Experimental Agrícola Fabio Baudrit Moreno (site code 84187). The observed modulation of the rainfall diurnal cycle is examined in the context of composite behavior of surface meteorological variables as well as the thermodynamic vertical structure preceding diurnal cycle development in relationship to TEW convective phase. Although we do not have long-term observations of critical boundary layer characteristics (e.g., boundary layer height), we infer how differences in boundary layer development and evolution with TEW phase may account for the observed diurnal modulation.

2. Data and Methods

We use 12:00 UTC soundings (06:00 LT) obtained from the University of Wyoming upper air sounding archive as well as hourly observations of rainfall and other meteorological variables (temperature, relative humidity, wind-speed, and wind direction) provided courtesy of the IMN. For the purposes of constructing composites, sounding profiles were linearly interpolated to common pressure levels starting at 900 mb and separated by 25 mb. Regarding quality control, soundings were rejected if either temperature or mixing ratio at a common pressure level was deemed a statistical outlier (i.e., outside of 3x the interquartile range) and if no profile data were available above 400 mb. Additionally, thermodynamic parameters indicative of the convective environment as estimated from the soundings (convective available potential energy, convective inhibition, and precipitable water) were extracted from the header of each sounding file.

To characterize forcing associated with TEWs, we use a spactime-filtered version of the twice daily $2.5^\circ \times 2.5^\circ$ National Oceanic and Atmospheric Administration (NOAA) outgoing longwave radiation (OLR) data set (Liebmann & Smith, 1996). The filtering scheme employed (see Wheeler and Kiladis (1999)) is designed to isolate westward propagating disturbances with timescales of 2–10 days and westward wavenumbers of 6–20 and has been shown previously to yield plausible TEW convective anomalies in the tropical eastern Pacific (Serra et al., 2008, 2010). Although we expect that TEWs account for much of the variability in this “tropical disturbance” (TD) band, it is likely that other types of variability (e.g., tropical cyclones or synoptic scale variability in the ITCZ) are captured as well. However, TD-filtered OLR has been applied in multiple studies of TEWs for which it has yielded results consistent with independent techniques for identifying TEWs (e.g., vorticity tracking, as considered in Serra et al. (2010) and Torres and Thorncroft (2022)).

Convectively active, suppressed, and neutral TEW phase conditions are defined from the standard deviation (σ) of TD-filtered OLR at the closest grid point to the sounding ($\sigma = 8.9 \frac{\text{W}}{\text{m}^2}$). That is, active (suppressed) phases correspond to TD-filtered OLR values less than (greater than) -1σ ($+1\sigma$), while neutral phases correspond to values between $\pm 1\sigma$. Note that different thresholds for defining TEW phase were assessed (e.g., between $\pm 1\sigma$ and $\pm 2\sigma$), with the results presented below qualitatively insensitive to the selected thresholds. Two separate analysis time intervals are considered, either 1979–2019 or 1995–2019, depending on the common availability of data. In particular, while soundings are available from 1973, OLR is available from 1979 and IMN hourly surface meteorology from 1995.

3. Results and Discussion

We begin by presenting an overview of the climatological mean seasonal and diurnal cycle characteristics of hourly IMN rainfall at SJO (Figure 1). Here we decompose rainfall as the product of a frequency of occurrence and a conditional intensity, that is, the hourly rainfall rate during rainy conditions, defined from the start of each hour (e.g., 00:00 LT corresponds to the 60 min period between 00:00 and 01:00 LT). We restrict consideration to

the wet season months over Costa Rica, May–November (MJJASON), which is also the period of the year during which TEWs are most active here (Roundy & Frank, 2004).

Several prominent features of the climatological rainfall behavior are evident. As evident in the seasonal evolution of both the frequency of occurrence (Figure 1a) and the mean daily rainfall accumulation (Figure 1c, black line), the wet season rainfall is double-peaked: for example, occurrence frequencies at or above 50% occur during a short first period extending from mid-May to mid-June and a longer, second period from early-mid September to late October, consistent with the findings of Durán-Quesada et al. (2020). The interval between these wet season peaks corresponds to the midsummer drought (MSD), or *veranillo* as it is referred to locally (Magaña et al., 1999). Although the MSD is a well-known climatological feature over the Pacific coast of Central America and Mexico, its cause remains a subject of debate (García-Franco et al., 2022). From the perspective of TEWs, it is noteworthy that the peak variability in the TD-filtered OLR index (Figure 1c, red line) occurs during the early part of the MSD.

Throughout MJJASON, the occurrence frequency (Figure 1a) exhibits fairly consistent rainfall initiation in the early afternoon hours; in the average over the entire wet season, the occurrence frequency peaks at 16:00 LT (Figure 1b, black line). During the peaks of the wet season, occurrence frequencies of 30% or more may persist into the evening, while during the MSD, rainfall frequencies are much lower at and following the diurnal peak (see Figure S2 in Supporting Information S1). Thus, there is broadening of the diurnal occurrence frequency peak over the evening hours during the rainiest intervals in the wet season. Climatological occurrence frequency between midnight and the morning hours at SJO is generally less than 10%; however, it may reach slightly higher values during the peaks of the wet season, which is consistent with storm size conditional convective rain rate behavior evident over the central domain of Costa Rica as shown by Rapp et al. (2014).

The MJJASON mean diurnal cycle of conditional intensity (Figure 1b, red line) exhibits a peak at 14:00 LT, or two hours earlier than the occurrence frequency. The difference in phasing between peak conditional intensity and occurrence frequency may reflect different types of rainfall (e.g., convective vs. stratiform) over the course of the diurnal cycle. While we have not explicitly explored the nature of the systems accounting for the diurnal rainfall behavior at SJO, peaking of conditional intensity before occurrence frequency is consistent with temporal evolution from more intense, convective rainfall to less intense, stratiform rainfall, a behavior often observed over the lifetime of MCSs (Biasutti & Yuter, 2013; Houze, 2004).

We next illustrate the diurnal cycle of wet season rainfall in relation to TEW convective phase estimated from TD-filtered OLR (Figure 2). The total rainfall (Figure 2a) exhibits a pronounced enhancement of active phase rainfall (red line) relative to the neutral (black) and suppressed (blue) phases, with a peak in hourly accumulation for the active phase approaching 2.0 mm, compared to ~1.4 and ~1.2 mm for the neutral and suppressed phases, respectively. Departures of active and suppressed phase rainfall from the neutral phase are most evident near and following the diurnal peak, as indicated by clear separation of the standard errors of the mean. For occurrence frequency by TEW phase (Figure 2b), active phase conditions manifest higher occurrence frequencies both before and after the diurnal peak. Although conditional intensity (Figure 2c) shows a tendency for higher values during active phases over the course of the diurnal cycle, the phase separation is less pronounced compared to the occurrence frequency (i.e., there is more overlap of the standard error of the mean). Interestingly, the diurnal maximum of conditional intensity in the suppressed phase is of comparable amplitude to the active phase; further, the peak seems to occur approximately 1 hr earlier relative to the active phase. Also notable in the conditional intensity are the larger nighttime to early morning values evident under active phase conditions, even as nighttime and early morning occurrence frequencies in both phases are comparable.

Overall, the results of the rainfall behavior illustrated in Figure 2 point to active TEW phases supporting enhanced rainfall relative to either convectively neutral or suppressed phases. The composite daily mean MJJASON rainfall accumulation is 10.1 mm in the active phase, compared to 7.9 and 6.7 mm in the neutral and suppressed phases, respectively. Throughout the diurnal cycle, TEW active phases are associated with more frequent occurrence of rainy conditions. On the other hand, the sensitivity of conditional intensity to TEW phase is somewhat more complicated, as peak diurnal intensity is comparable during the active and suppressed phases, but with some indication of phase shifting. The effect of TEW convective phase on SJO rainfall described here is broadly consistent with previous studies attributing tropical rainfall variability to changes in frequency rather than intensity (Morrissey et al., 1994). For example, a study by Li et al. (2020) on El Niño/Southern Oscillation modulation

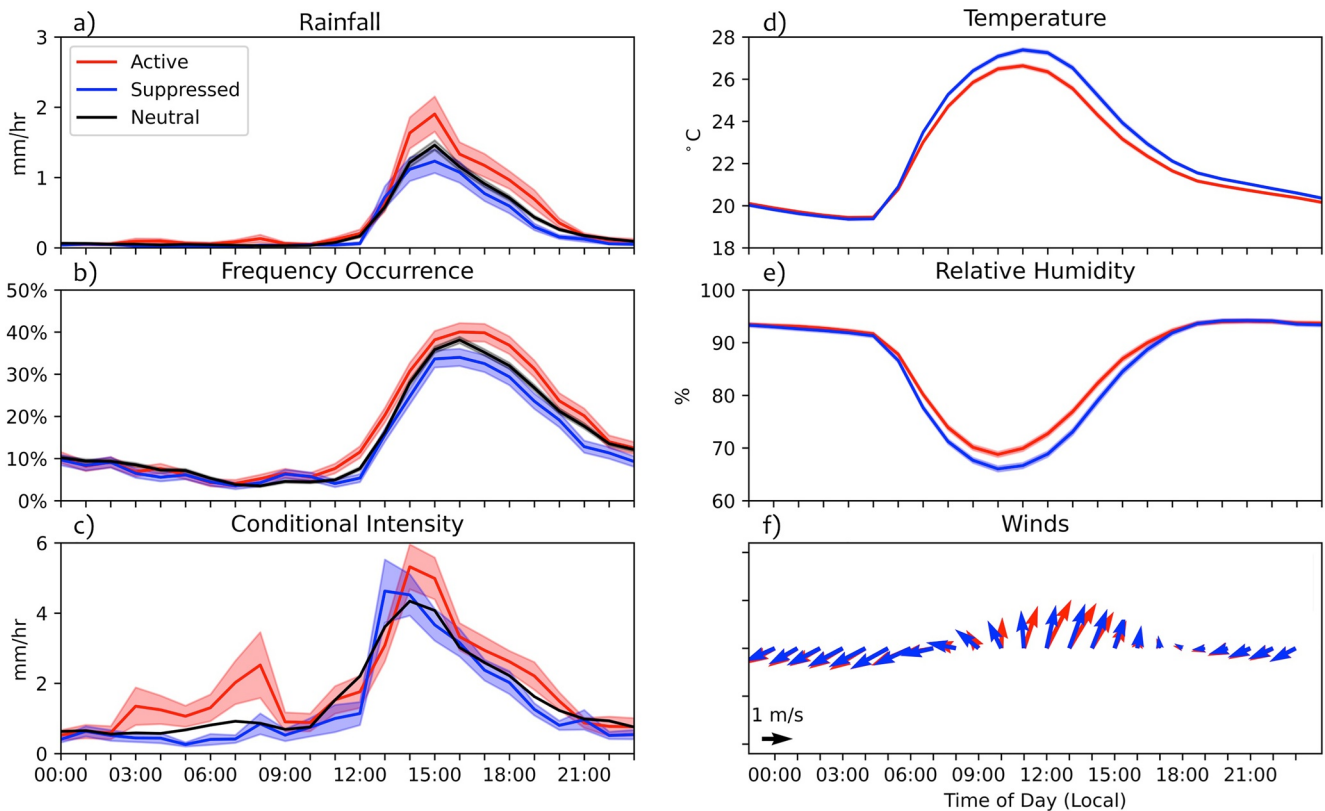


Figure 2. Composite diurnal cycles for TD-outgoing longwave radiation active and suppressed phases during May–November (1995–2019). (a) Rainfall (in mm/hr); (b) Occurrence frequency (in percent); (c) Conditional intensity (in mm/hr); (d) Air temperature (in °C); (e) Relative humidity (in percentage); and (f) Winds (in m/s, with arrows oriented in the direction of the wind, with north at the top and east to the right). Active phase is in red, suppressed phase in blue; panels (a–c) also include the neutral phase for comparison. In panels (a–e), shading corresponds to standard errors of each phase mean.

of tropical rainfall using subdaily satellite and rain gauge data found a stronger impact on rainfall frequency than intensity.

Fundamentally, the robustness of the rainfall diurnal cycle—the fact that a clear afternoon peak is present in both convectively active and suppressed TEW phases—underscores the leading-order importance of coupling of precipitating deep convection to the land surface at the observation site. Of course, TEWs may modulate the near surface environment, so it is worth exploring the extent to which TEW convective phase sensitivity is evident in surface meteorological variables, and how such sensitivity may be expected to impact diurnal rainfall behavior. To this end, Figures 2d–2f depict diurnal cycles of air temperature, relative humidity, and wind, respectively.

Relative to TEW suppressed phase conditions, active phases feature cooler near surface air temperatures (Figure 2d), especially around mid-day, with higher relative humidity (Figure 2e). The cooler, moister boundary layer environment during active phases is associated with a modest mean lowering (~50 m) of the lifting condensation level (LCL; not shown) between active and suppressed phases. Active phase lowering of the LCL may be expected to promote lowering of cloud base. On the other hand, reduced morning time active phase heating of the surface, arising through, for example, reduced net surface shortwave under cloudier active phase conditions, may be expected to slow the development of a vigorous, deep, well-mixed daytime boundary layer, with the latter conducive to land region transition to deep convection (Yano, 2021). This effect may account for the one-hour delay evident in active phase conditional intensity (Figure 2b) compared to the suppressed phase.

The near surface zonal and meridional winds (Figure 2f) also indicate some sensitivity to TEW phase, with more southwesterly conditions favored during the late morning and early afternoon of active phases. That is, TEW active phases promote an enhancement in the diurnal evolution of winds at the observation site, which exhibit a partial reversal in direction between the daytime and nighttime hours (Mora et al., 2020). This behavior may be indicative of a local mountain-valley breeze circulation, with daytime upsloping (southerly/southwesterly)

flow toward the higher topography to the north and east of SJO (see Figure S1 in Supporting Information S1). We speculate that enhanced active phase convection over topography to the northeast could act to reinforce the mountain-valley breeze circulation, although more observations would be needed to confirm this idea.

Although the diurnal cycle of rainfall at the SJO site appears to be tied to the surface, it is not solely dependent on the surface conditions. Considering how free tropospheric conditions may influence moist convection over land, for instance, Gentine et al. (2013) employed a slab boundary layer model to demonstrate how free tropospheric stability and moisture interact with surface forcing to affect whether dry or moist land surface states are more favorable to precipitating deep convection. Although such comprehensive mechanistic attribution is beyond the scope of this study, we consider how the observed morningtime (12:00 UTC/06:00 LT) composite sounding characteristics for active and suppressed phases may act to constrain boundary layer and subsequent convective development from above (Figure 3). Free tropospheric conditions may evolve over the course of diurnal cycle development; in fact, in the case of TEWs, which have a period of about 4 days (e.g., Tai & Ogura, 1987), the phase progression may be sufficiently rapid that free tropospheric conditions could vary appreciably over a single diurnal cycle, which should be kept in mind when interpreting our results.

Figure 3 presents composited sounding profiles of temperature, mixing ratio, and meridional wind for active minus suppressed phase conditions. Note that of the 3,691 soundings retained for the period 1979–2019, 383 (~10.4%) are classified as active phase, 389 (~10.5%) as suppressed phase soundings, and 2,919 (~79.1%) as neutral phase soundings according to the TD-filtered OLR. In addition to showing composite differences based on the 06:00 LT soundings of identified active and suppressed phase days ($t = 0$), we show lead and lag composite differences based on available soundings from 48 hr before ($t = -48$) to 48 hr ($t = +48$) after the peak phase anomaly at the site. The temperature profile at $t = 0$ indicates anomalously cool conditions below and warm conditions aloft. At the same time, anomalous active minus suppressed phase moistening is present over a deep layer extending from the surface to 300 mb. Meridional winds at $t = 0$ are weakly southerly over much of the troposphere. The lead/lag behavior depicted captures the phase progression expected with the passage of TEWs. For example, the meridional winds aloft at $t = -24$ are northerly followed by southerlies aloft at $t = +24$; thus, conditions at $t = 0$ are consistent with a trough. The composited phase differences are also consistent with prior analyses of the vertical structures of TEWs in the region (e.g., Serra et al., 2010). It is worth noting the tilt of the anomalous moistening with height, with elevated values aloft present at $t = +24$, suggestive of convective moistening of the atmospheric column within the active phase of the waves typical of convectively coupled waves (e.g., Kiladis et al., 2009; Serra et al., 2008, 2010). While we do not show them here, composite differences for active minus neutral and suppressed minus neutral conditions reflect anomalies that are largely opposite to one another, that is, the phase sensitivity is effectively linear.

To summarize the behavior of several simple sounding-derived diagnostics of the convective environment—namely convective available potential energy (CAPE), convective inhibit (CIN), and precipitable water vapor (PWV)—during TD-OLR active and suppressed phases, we present scatterplots of the quantile distributions (QQ-plots) of these diagnostics for the two phases (Figure 4). That is, the values of each diagnostic depicted in Figure 4 are, for each phase, first sorted from smallest to largest, and then the sorted distributions are sampled at specified quantiles; the resultant scatterplots are formed by plotting the pair of active and suppressed phase values at each quantile. Morningtime CAPE (Figure 4a) deviates markedly from the 1:1 line, with values at a given quantile typically twice as large for active phases compared to suppressed phases, indicating that the former have more potential energy present in the morningtime environment to support subsequent precipitating diurnal deep convection. The CIN magnitudes are smaller in the active phase over much of the characteristic range, although as CIN approaches zero, active phase CIN quantile values are somewhat larger. In other words, while the energetic barrier that needs to be overcome for diurnal rainfall to occur is often lower during TEW active phases, there may be instances for which the initial conditions present in suppressed phases are more conducive to convection, at least in the sense of a smaller CIN barrier.

The 06:00 LT PWV values during the active phase are generally 2–3 mm higher than during the suppressed phase, consistent with the deep layer mixing ratio anomalies evident in the composited soundings. Previous work (e.g., Holloway & Neelin, 2009; Schiro et al., 2016) has quantified the relationship between PWV and rainfall in the tropics, with the former viewed as a proxy for conditional instability. Here, we find qualitatively that the relatively moister conditions prevailing over much of the troposphere during the mornings for active phase days provides a more significant “reservoir” of water vapor for rainfall; indeed, the characteristic differences in PWV values are quantitatively consistent with the active minus suppressed phase differences reported above for daily mean rainfall accumulation. Furthermore, moistening over a deep layer may be expected to provide a more

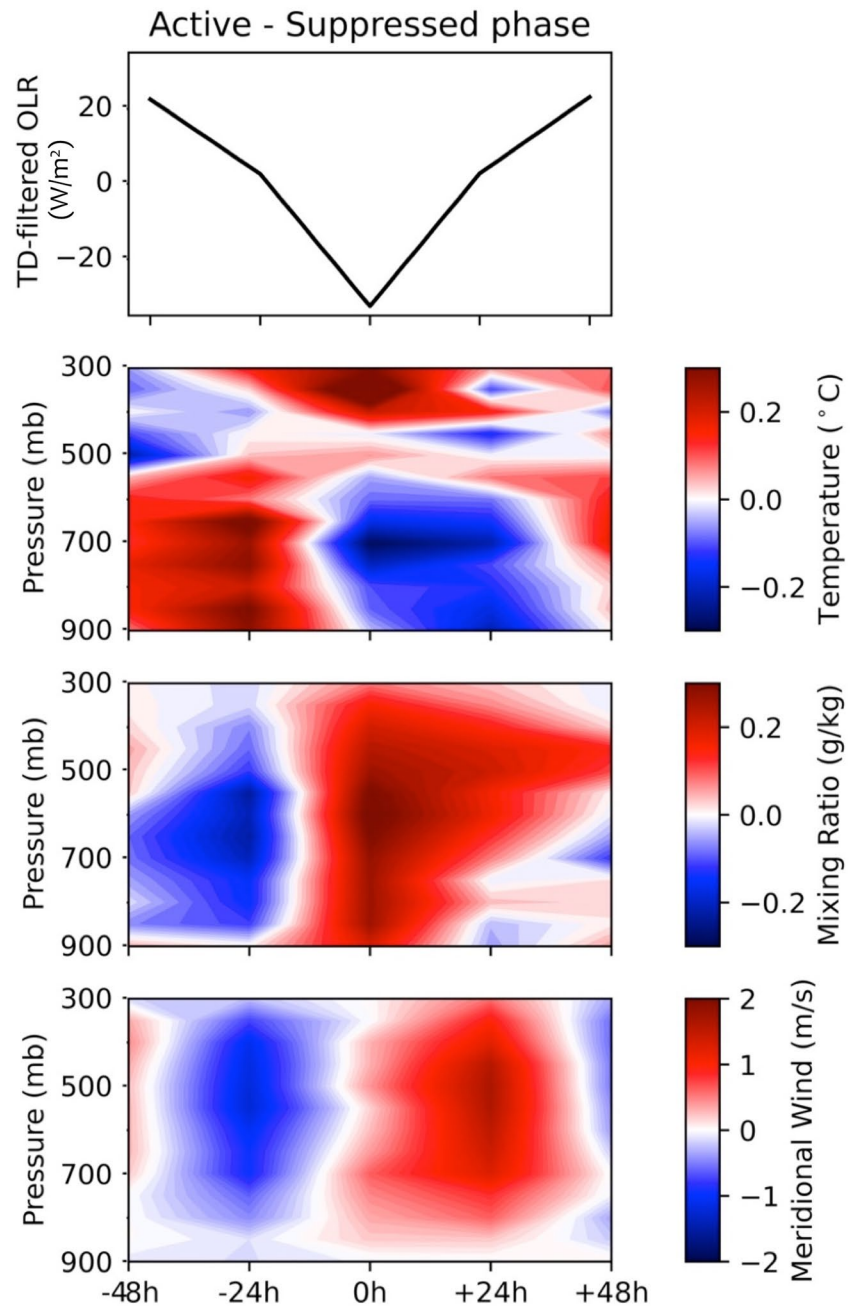


Figure 3. Lead/lag tropical easterly wave convectively active minus suppressed phase composites based on the morningtime (06:00 LT) soundings at SJO (1979–2019). The TD-outgoing longwave radiation index for active minus suppressed phases (in W m^{-2}) is shown at the top, along with temperature (in $^{\circ}\text{C}$), mixing ratio (in g kg^{-1}), and meridional wind (in m s^{-1}) composites by pressure levels.

conductive environment for diurnal deep convective development by, for example, mitigating dry air entrainment in the free troposphere that may reduce buoyancy or increase stability.

4. Summary and Conclusions

Using two decades of surface meteorology observations co-located with the WMO sounding site near San José, Costa Rica, we have presented evidence of modulation of the local diurnal cycle of rainfall by TEWs. Principally, we find an enhanced likelihood of occurrence of rainfall during TEW active phases compared to neutral

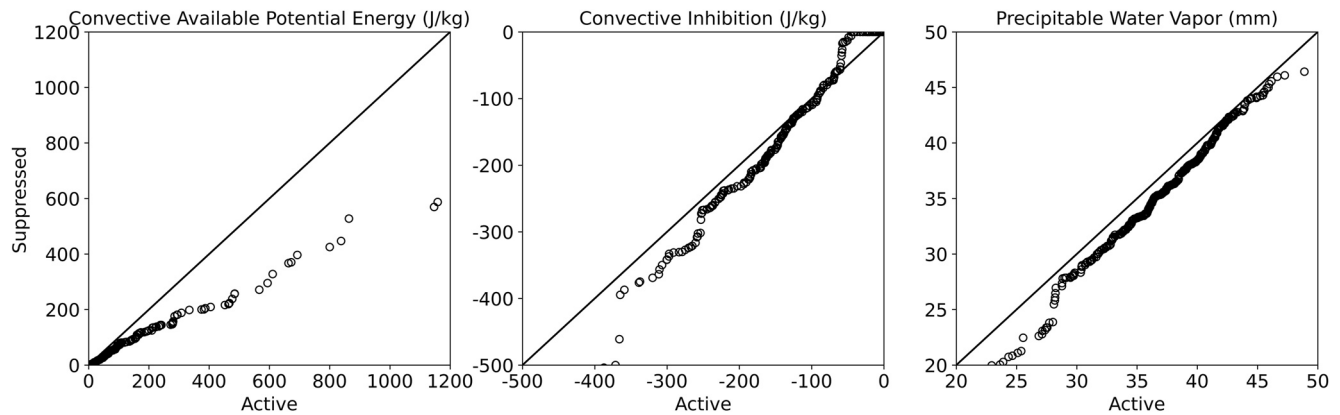


Figure 4. Quantile-quantile plots of SJO 06:00 LT sounding thermodynamic parameters for tropical easterly wave active versus suppressed phase conditions (1979–2019). (a) Convective available potential energy (in J/kg); (b) Convective inhibition (in J/kg); and (c) Precipitable water vapor (in mm).

and suppressed phases. Regarding rainfall intensity, peak mean hourly rainfall is comparable for the active and suppressed phases. However, active phase conditions are associated with a slightly delayed peak, along with higher intensity on the descending (evening) side of the diurnal peak.

Analysis of surface meteorological variables indicates a cooler and moister surface over the course of the diurnal cycle for TEW active phase conditions. At the same time, the morning time soundings and derived thermodynamic parameters point to greater instability (higher CAPE), a smaller barrier for convective initiation (lower CIN), and an enhanced reservoir of moisture to sustain rainfall (higher PWV) during active phases, consistent with TEW modulation of vertical thermodynamic profiles. Thus, both near surface conditions and vertical profile thermodynamics appear to play a role in shaping how TEWs modulate diurnal rainfall at the observing site.

Better understanding of the coupling between the diurnal cycle and TEWs may have important implications for predicting or forecasting extreme event impacts over Costa Rica (and the tropical Americas more broadly). As previously noted, IMN often generates forecast advisories for extreme rainfall with TEW passage, though the occurrence of heavy rainfall may be highly variable. We hypothesize that the timing of TEW occurrence relative to the phasing of the diurnal cycle may account for some of the differential rainfall impact, particularly in terms of extremes, although evaluating this hypothesis from observations requires more detailed treatment of wave phase (at sufficiently high temporal resolution) and consideration of the location and spatial extent of the wave with respect to a given observation site. On the other hand, it may be possible to use regional model frameworks that adequately capture TEW-precipitation relationships over land to investigate how the rainfall response to TEW forcing depends on diurnal phasing. We further emphasize the need for continued, comprehensive in situ monitoring to diagnose TEW modulation of tropical land-region rainfall more precisely, particularly to the extent that this may enhance early warning capacity.

Data Availability Statement

WMO sounding data (site #78762) were downloaded from the University of Wyoming upper air sounding archive website at <https://weather.uwyo.edu/upperair/sounding.html>. Hourly surface meteorology data (including precipitation, air temperature, relative humidity, windspeed, and wind direction) from Estación Experimental Agrícola Fabio Baudrit Moreno (site #84187) were provided by the Instituto Meteorológico Nacional de Costa Rica and can be requested via <https://www.imn.ac.cr/web/imn/solicitud-de-servicios>. (Data requests should include reference to Ana María Durán-Quesada [ana.duranquesada@ucr.ac.cr] and data contract IMN-DIM-044-2023.) Twice-daily outgoing longwave radiation data were provided by Dr. George Kiladis of the NOAA Physical Sciences Laboratory (george.kiladis@noaa.gov), and the data file ([olr.2xdaily.1979-2022.nc](https://downloads.psl.noaa.gov/Datasets/interp_OLR/)) can be downloaded from https://downloads.psl.noaa.gov/Datasets/interp_OLR/.

Acknowledgments

The authors acknowledge provision of Instituto Meteorológico Nacional surface hourly meteorological observations under data Contract IMN-DIM-044-2023. RMW acknowledges funding support provided by a graduate assistantship through the Rutgers Institute of Earth, Ocean, and Atmospheric Sciences. YLS acknowledges support of National Science Foundation Grant AGS-1758666.

References

Biasutti, M., & Yuter, S. E. (2013). Observed frequency and intensity of tropical precipitation from instantaneous estimates. *Journal of Geophysical Research: Atmospheres*, 118(17), 9534–9551. <https://doi.org/10.1002/jgrd.50694>

Dominguez, C., Done, J. M., & Bruyère, C. L. (2020). Easterly wave contributions to seasonal rainfall over the tropical Americas in observations and a regional climate model. *Climate Dynamics*, 54(1–2), 191–209. <https://doi.org/10.1007/s00382-019-04996-7>

Durán-Quesada, A. M., Sorí, R., Ordoñez, P., & Gimeno, L. (2020). Climate perspectives in the intra–Americas seas. *Atmosphere*, 11(9), 959. <https://doi.org/10.3390/atmos11090959>

Fuchs-Stone, Z., Raymond, D. J., & Sentić, S. (2020). OTREC2019: Convection over the East Pacific and southwest Caribbean. *Geophysical Research Letters*, 47(11), e2020GL087564. <https://doi.org/10.1029/2020GL087564>

Fuller, R., & Stensrud, D. (2000). The relationship between tropical easterly waves and surges over the Gulf of California during the North American monsoon. *Monthly Weather Review*, 128(8), 2983–2989. [https://doi.org/10.1175/1520-0493\(2000\)128<2983:trbtew>2.0.co;2](https://doi.org/10.1175/1520-0493(2000)128<2983:trbtew>2.0.co;2)

García-Franco, J. L., Chadwick, R., Gray, L. J., Osprey, S., & Adams, D. K. (2022). Revisiting mechanisms of the Mesoamerican midsummer drought. *Climate Dynamics*, 60(1–2), 549–569. <https://doi.org/10.1007/s00382-022-06338-6>

Gentine, P., Holtslag, A. A. M., D’Andrea, F., & Ek, M. (2013). Surface and atmospheric controls on the onset of moist convection over land. *Journal of Hydrometeorology*, 14(5), 1443–1462. <https://doi.org/10.1175/jhm-d-12-0137.1>

Giraldo-Cardenas, S., Arias, P. A., Vieira, S. C., & Zuluaga, M. D. (2022). Easterly waves and precipitation over northern South America and the Caribbean. *International Journal of Climatology*, 42(3), 1483–1499. <https://doi.org/10.1002/joc.7315>

Gomes, H. B., Ambrizzi, T., Pontes da Silva, B. F., Hodges, K., Silva Dias, P. L., Herdies, D. L., et al. (2019). Climatology of easterly wave disturbances over the tropical South Atlantic. *Climate Dynamics*, 53(3–4), 1393–1411. <https://doi.org/10.1007/s00382-019-04667-7>

Higgins, R. W., Shi, W., & Hain, C. (2004). Relationships between Gulf of California moisture surges and precipitation in the southwestern United States. *Journal of Climate*, 17(15), 2983–2997. [https://doi.org/10.1175/1520-0442\(2004\)017<2983:rbgocm>2.0.co;2](https://doi.org/10.1175/1520-0442(2004)017<2983:rbgocm>2.0.co;2)

Holloway, C. E., & Neelin, J. D. (2009). Moisture vertical structure, column water vapor, and tropical deep convection. *Journal of the Atmospheric Sciences*, 66(6), 1665–1683. <https://doi.org/10.1175/2008jas2806.1>

Hopsch, S. B., Thorncroft, C. D., & Tyle, K. R. (2010). Analysis of African easterly wave structures and their role in influencing tropical Cyclogenesis. *Monthly Weather Review*, 138(4), 1399–1419. <https://doi.org/10.1175/2009MWR2760.1>

Houze, R. A. (2004). Mesoscale convective systems. *Reviews of Geophysics*, 42(4), RG4003. <https://doi.org/10.1029/2004RG000150>

Huaman, L., Schumacher, C., & Sobel, A. H. (2022). Assessing the vertical velocity of the east Pacific ITCZ. *Geophysical Research Letters*, 49(1), e2021GL096192. <https://doi.org/10.1029/2021gl096192>

IMN. (2023). Avisos Meteorológicos [online]. Retrieved from <https://www.imn.ac.cr/web/imn/avisos-meteorologicos>

Jury, M. R. (2020). Resolution-dependent perspectives on Caribbean hydro-climate change. *Hydrology*, 7(4), 93. <https://doi.org/10.3390/hydrology7040093>

Kiladis, G. N., Wheeler, M. C., Haertel, P. T., Straub, K. H., & Roundy, P. E. (2009). Convectively coupled equatorial waves. *Reviews of Geophysics*, 47(2), RG2003. <https://doi.org/10.1029/2008RG000266>

Li, X. F., Blenkinsop, S., Barbero, R., Yu, J., Lewis, E., Lenderink, G., et al. (2020). Global distribution of the intensity and frequency of hourly precipitation and their responses to ENSO. *Climate Dynamics*, 54(11–12), 4823–4839. <https://doi.org/10.1007/s00382-020-05258-7>

Liebmann, B., & Smith, C. A. (1996). Description of a complete (interpolated) outgoing longwave radiation data set. *Bulletin American Meteorology Society*, 77, 1275–1277.

Liu, C., & Zipser, E. J. (2008). Diurnal cycles of precipitation, clouds, and lightning in the tropics from 9 years of TRMM observations. *Geophysical Research Letters*, 35(4), L04819. <https://doi.org/10.1029/2007GL032437>

Magaña, V., Amado, J. A., & Medina, S. (1999). The midsummer drought over Mexico and Central America. *Journal of Climate*, 12(6), 1577–1588. [https://doi.org/10.1175/1520-0442\(1999\)012<1577:tmddmra>2.0.co;2](https://doi.org/10.1175/1520-0442(1999)012<1577:tmddmra>2.0.co;2)

Mapes, B. E., Warner, T. T., & Xu, M. (2003). Diurnal patterns of rainfall in Northwestern South America. Part III: Diurnal gravity waves and nocturnal convection offshore. *Monthly Weather Review*, 131(5), 830–844. [https://doi.org/10.1175/1520-0493\(2003\)131<0830:dporin>2.0.co;2](https://doi.org/10.1175/1520-0493(2003)131<0830:dporin>2.0.co;2)

Mapes, B. E., Warner, T. T., Xu, M., & Negri, A. J. (2003). Diurnal patterns of rainfall in Northwestern South America. Part I: Observations and context. *Monthly Weather Review*, 131(5), 799–812. [https://doi.org/10.1175/1520-0493\(2003\)131<0799:dporin>2.0.co;2](https://doi.org/10.1175/1520-0493(2003)131<0799:dporin>2.0.co;2)

Mekonnen, A., Thorncroft, C. D., & Aiyyer, A. R. (2006). Analysis of convection and its association with African easterly waves. *Journal of Climate*, 19(20), 5405–5421. <https://doi.org/10.1175/jcli3920.1>

Mora, N., Amador, J. A., Rivera, E. R., & Maldonado, T. (2020). A sea breeze study during Ticosonde-NAME 2004 in the central Pacific of Costa Rica: Observations and numerical modeling. *Atmosphere*, 11(12), 1333. <https://doi.org/10.3390/atmos11121333>

Morrissey, M. L., Krajewski, W. F., & McPhaden, M. J. (1994). Estimating rainfall in the tropics using the fractional time raining. *Journal of Applied Meteorology*, 33(3), 387–393. [https://doi.org/10.1175/1520-0450\(1994\)033<0387:erittu>2.0.co;2](https://doi.org/10.1175/1520-0450(1994)033<0387:erittu>2.0.co;2)

Nesbitt, S. W., & Zipser, E. J. (2003). The diurnal cycle of rainfall and convective intensity according to three years of TRMM measurements. *Journal of Climate*, 16(10), 1456–1475. <https://doi.org/10.1175/1520-0442-16.10.1456>

Rapp, A. D., Peterson, A. G., Frauenfeld, O. W., Quiring, S. M., & Roark, E. B. (2014). Climatology of storm characteristics in Costa Rica using the TRMM precipitation radar. *Journal of Hydrometeorology*, 15(6), 2615–2633. <https://doi.org/10.1175/jhm-d-13-0174.1>

Roundy, P. E., & Frank, W. (2004). A climatology of waves in the equatorial region. *Journal of the Atmospheric Sciences*, 61(17), 2105–2132. [https://doi.org/10.1175/1520-0469\(2004\)061<2105:acowit>2.0.co;2](https://doi.org/10.1175/1520-0469(2004)061<2105:acowit>2.0.co;2)

Rydbeck, A. V., & Maloney, E. D. (2014). Energetics of East Pacific easterly waves during intraseasonal events. *Journal of Climate*, 27(20), 7603–7621. <https://doi.org/10.1175/jcli-d-14-00211.1>

Rydbeck, A. V., & Maloney, E. D. (2015). On the convective coupling and moisture organization of East Pacific easterly waves. *Journal of the Atmospheric Sciences*, 72(10), 3850–3870. <https://doi.org/10.1175/jas-d-15-0056.1>

Schiro, K. A., Neelin, J. D., Adams, D. K., & Lintner, B. R. (2016). Deep convection and column water vapor over tropical land versus tropical ocean: A comparison between the Amazon and the tropical western Pacific. *Journal of the Atmospheric Sciences*, 73(10), 4043–4063. <https://doi.org/10.1175/JAS-D-16-0119.1>

Seastrand, S., Serra, Y. L., Castro, C., & Ritchie, E. A. (2015). The dominant synoptic-scale modes of North American monsoon precipitation. *International Journal of Climatology*, 35(8), 2019–2032. <https://doi.org/10.1002/joc.4104>

Serra, Y. L., Kiladis, G. N., & Cronin, M. F. (2008). Horizontal and vertical structure of easterly waves in the Pacific ITCZ. *Journal of the Atmospheric Sciences*, 65(4), 1266–1284. <https://doi.org/10.1175/2007JAS2341.1>

Serra, Y. L., Kiladis, G. N., & Hodges, K. I. (2010). Tracking and mean structure of easterly waves over the intra-Americas sea. *Journal of Climate*, 23(18), 4823–4840. <https://doi.org/10.1175/2010JCLI3223.1>

- Tai, K.-S., & Ogura, Y. (1987). An observational study of easterly waves over the eastern Pacific in the northern summer using FGGE data. *Journal of the Atmospheric Sciences*, *44*(2), 339–361. [https://doi.org/10.1175/1520-0469\(1987\)044<0339:aosow>2.0.co;2](https://doi.org/10.1175/1520-0469(1987)044<0339:aosow>2.0.co;2)
- Thorncroft, C., & Hodges, K. (2001). African easterly wave variability and its relationship to Atlantic tropical cyclone activity. *Journal of Climate*, *14*(6), 1166–1179. [https://doi.org/10.1175/1520-0442\(2001\)014<1166:aewvai>2.0.co;2](https://doi.org/10.1175/1520-0442(2001)014<1166:aewvai>2.0.co;2)
- Torres, V. M., & Thorncroft, C. D. (2022). Analysis of the environment that supports easterly waves over the eastern Pacific and the intra-Americas sea in the boreal summer—A potential vorticity perspective. *Journal of Climate*, *35*(12), 3961–3977. <https://doi.org/10.1175/jcli-d-21-0482.1>
- Warner, T. T., Mapes, B. E., & Xu, M. (2003). Diurnal patterns of rainfall in Northwestern South America. Part II: Model simulations. *Monthly Weather Review*, *131*(5), 813–829. [https://doi.org/10.1175/1520-0493\(2003\)131<0813:dporin>2.0.co;2](https://doi.org/10.1175/1520-0493(2003)131<0813:dporin>2.0.co;2)
- Wheeler, M., & Kiladis, G. (1999). Convectively coupled equatorial waves: Analysis of clouds and temperature in the wavenumber-frequency domain. *Journal of the Atmospheric Sciences*, *56*(3), 374–399. [https://doi.org/10.1175/1520-0469\(1999\)056<0374:ccewao>2.0.co;2](https://doi.org/10.1175/1520-0469(1999)056<0374:ccewao>2.0.co;2)
- Yang, G.-Y., & Slingo, J. (2001). The diurnal cycle in the tropics. *Monthly Weather Review*, *129*(4), 784–801. [https://doi.org/10.1175/1520-0493\(2001\)129<0784:tdcitt>2.0.co;2](https://doi.org/10.1175/1520-0493(2001)129<0784:tdcitt>2.0.co;2)
- Yano, J.-I. (2021). Initiation of deep convection through deepening of well-mixed boundary layer. *The Quarterly Journal of the Royal Meteorological Society*, *147*(739), 3085–3095. <https://doi.org/10.1002/qj.4117>